Efficient and full-wave electromagnetic analysis of MRI antennas using the Array Scanning Method

J. Ignacio Echeveste[1], Denis Tihon[1], Marc Dubois[2], Redha Abdeddaim[2], Stefan Enoch[2], Christophe Craeye[1]
[1]Université catholique de Louvain: ICTEAM, Louvain-la-Neuve, Belgium, jose.echeveste@uclouvain.be
[2]Aix Marseille Univ., CNRS, Centrale Marseille, Institut Fresnel, Marseille, France

***Abstract*—The electromagnetic analysis involved in magnetic resonance imaging scanners is becoming more challenging. The wavelength of the RF-pulse is continuously decreasing as the static magnetic field is increased, looking for an enhancement of the MRI performance. The scanners are getting more complex as they are now composed of multiple receiving and transmitting antennas. Furthermore, the inclusion of metamaterials and metasurfaces are nowadays under study, looking for an homogenization of the RF magnetic fields. Efficient and accurate electromagnetic tools for the analysis and design of complex High-Field and Ultra High-Field MRI antennas is required. In this work, an efficient analysis tool based on the method of moments and on the array scanning method is proposed. Fully representative designs are studied, and results are compared with commercial software.**

Keywords: Antenna, magnetic resonance imaging, method of moments, array scanning method, birdcage coil.

I. Introduction

Magnetic resonance imaging (MRI) is a well-known technique for obtaining human or animal body images in vivo; it is based on the nuclear magnetic resonance successfully studied and measured in the seminal works of Bloch and Purcell [1], [2]. One of the advantages of this technique is that it is non-invasive. To improve the quality of the images obtained with MRI, the magnetic flux densities is increased, from lower than 1 Tesla at first [3] to MRI machines working at 7, 11.7, 17 and even 21 Tesla nowadays. Only MRI machines working up to 11.7 Tesla have been used on humans so far due to the large volume over which the magnetic field must be generated. The other MRI machines are dedicated to the study of small animals. The increase in the static magnetic flux density directly implies an increase in the working frequency, both being related through the gyromagnetic ratio. Other approaches that are currently being under study, such as parallel transmission (pTx) [4], consist in the use of an array of antennas for transmitting or receiving the radio-frequency pulses. Furthermore, metamaterials or metasurfaces have recently been considered to homogenize the RF magnetic fields [5], [6]. All these improvements require more complex systems and consequently the electromagnetic analysis becomes more difficult and also computationally more expensive. Therefore, efficient and accurate electromagnetic tools for the analysis and design of MRI systems is of great importance on the way toward high quality images without blind spots.

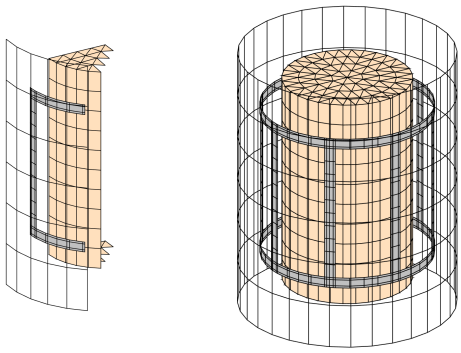

(a) Unit cell (b) Complete mesh

Fig. 1: Representation of a common MRI scanner. Metallic tunnel used for RF-shielding, birdcage and dielectric phantom to compute the effects of a human body part.

The electromagnetic analysis of MRI scanners has quickly evolved in recent years. Birdcage coils were analyzed at first using equivalent-circuit analysis [7]. The effects of shielding were also efficiently studied and included in the design [8]. More accurate numerical methods are also used, such as the method of moments [9], [10], or hybrid methods that pursue efficiency [11].

Periodic constraints are usually employed in array antennas. Planar arrays are efficiently analyzed applying the infinite array approach, reducing in that way the analysis to one unit cell. Although the results obtained using this approximation are generally good, they are not exact, due to the finiteness of the original array. However, exact results are obtained if a similar technique is applied to structures that have an axial symmetry of revolution [12], such as circular arrays [13] or MRI scanners such as the one shown in Fig. 1. Indeed, such structures, sometimes called discrete volumes of revolution, are truly infinitely periodic with respect to the revolution angle.

In this work, an efficient and accurate analysis of MRI systems is presented. Taking into account the inherent symmetry of MRI scanners, the Array Scanning Method (ASM) [14], [15], [16] is employed to significantly reduce the computation time without affecting the accuracy. This approach is extended here to the treatment of dielectric objects, through the PM-CHWT formulation [17]. The reduction in time is directly related to the periodicity of the structure.

II. Array Scanning Method Analysis

The analysis of infinite periodic structures is usually limited to one unit cell. It is a common practice in the analysis of large array of antennas or metamaterials. In these cases the excitation of the structure is also periodized. Using the ASM, a non-periodic excitation is decomposed into a sum of quasi-periodic excitations, allowing one to analyze the response of a periodic structure to the non-periodic excitation. Considering an infinite linear array of elements with just one element excited and the others passively terminated. The current on any element can be computed as

$$I(n) = \frac{1}{2\pi} \int_0^{2\pi} I^{\infty}(\psi) e^{-jn\psi} d\psi \tag{1}$$

with $I(n)$ the total current on the n^{th} element and $I^{\infty}(\phi)$ the current on element 0 for the infinite array solution with phase shift of ϕ between consecutive elements [16]. Equation (1) can be simplified in the case of discrete volumes of revolution noticing that the excitation is periodic of period 2π with respect to the revolution angle. It leads to the discrete Fourier transform

$$I(n) = \frac{1}{N} \sum_{p=0}^{N-1} I^{\infty}(\psi_p) e^{-jm\psi_p} \tag{2}$$

This characteristic makes the ASM especially interesting for analyzing the radio-frequency antennas that are usually employed in MRI. Arrays of dipoles or coils, birdcages and metallic shielding are efficiently analyzed with the ASM. Phantoms that are usually approximated by cylindrical or spherical geometries can also be analyzed with the present method. Furthermore, metamaterials and metasurfaces that are currently being under study to enhance the MRI performances can also be modeled using this method, avoiding very computationally expensive problems. The method of moments based analysis of an array of antennas usually requires the solution of a problem of $(N \times M)$ by $(N \times M)$ system of equations, being N the number of antennas and M the number of basis functions per antenna. Applying the ASM, the $(N \times M)$ by $(N \times M)$ system of equations is decomposed into N independent M by M system of equations that can be solved separately. It leads to an acceleration of the filling time by a factor of N and of the brute-force solution time by a factor of N^2.

In this paper, we use the Poggio-Miller-Chu-Harrington-Wu-Tsai (PMCHWT) formulation of the method of moments [17]. This formulation allows for the simulation of penetrable bodies. The method consists in finding equivalent electric and magnetic currents along the interface between different media, such that the fields radiated by the currents correspond to the fields scattered by the structure. First, the surfaces are discretized using basis and testing functions. The unknown equivalent currents on the surfaces are expressed as a weighted sum of these basis functions. In order to find the weights, the continuity of the tangential fields along the interface is imposed along the testing functions in an averaged sense. It results into a system of equations of the type $Z \cdot x = -b$, with x the unknown weights, b the external excitation tested on the testing functions and Z the impedance matrix of the system. In the case of periodic structure with an order N symmetry, the bloc circulant structure of Z allows for a filling time that is N times reduced. Moreover, the problem can be decomposed with a $N \log(N)$ complexity into N independent systems of equations, decreasing the complexity of the solution from N^3 to $N \log(N)$ [12].

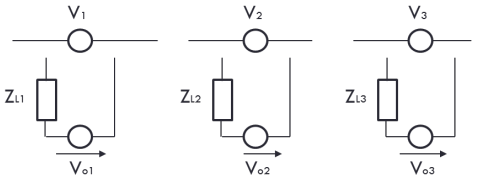

Fig. 2: Short-circuited analysis of an antenna array.

There are MRI elements, such as birdcages, that physically have an axial symmetry that is not shared by the excitation. This case can also be analyzed with the ASM with a simple post processing step. As an example, the high-pass birdcage coil [7], shown in Fig. 1, has 8 legs but just two of them have an excitation port. Applying symmetry restrictions and analyzing just the unit cell, then 8 ports are considered when actually only 2 are present. The elements are analyzed considering short-circuited antennas, as shown in Fig. 2. Then the actual loads or ports are included

$$V = Z(Z + Z_L)^{-1} V_0 \tag{3}$$

with V being the actual voltages that appears on the elements due to the application of an excitation vector V_0 (see generators in Fig. 2), Z is the mutual impedance matrix and Z_L is a diagonal matrix with the the values of the load impedance in each port. If the excitation and the load impedances are set to a null value then it is equivalent to not having any port, which is the case of most of the legs of a birdcage.

III. Validation

Several coils have been studied for MRI applications: dipoles, Helmholtz coils, saddle coils or birdcage coils are some of them.

The transverse magnetic field generated by these antennas can be decomposed according to circular polarizations: the $B_1^+ = B_x + jB_y$ and $B_1^- = B_x - jB_y$ fields. The former is used for proton excitation, while the latter is used for detection of the re-emitted signal. Birdcage coils are very popular as transmit coils since the B_1^+ field can be made homogeneous over wide volumes, while keeping the B_1^- field low. It is achieved by properly tuning the relative position and phase of the ports. Two examples are studied in this work. In the first one, a high-pass birdcage is analyzed. In the second example, the same birdcage is analyzed together with a dielectric phantom and a metallic shield that represents the MRI tunnel.

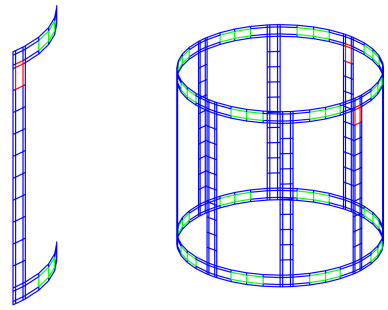

(a) Unit cell (b) Complete mesh

Fig. 3: Mesh of the example III.A. In red the basis functions in which the excitation is performed, in green the basis functions in which the capacitors are designed.

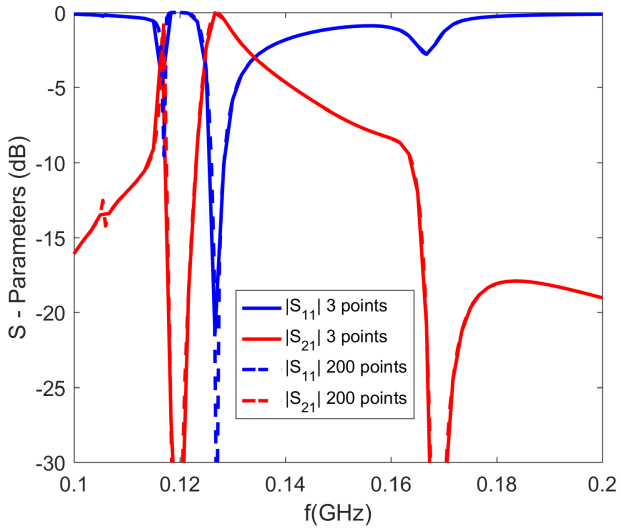

Fig. 4: Comparison of the scattering parameters of the birdcage coil of Section III.A. They are computed twice. First, the impedance matrices are computed just at three frequencies and then interpolated. Second, the impedance matrices are computed at 200 frequencies.

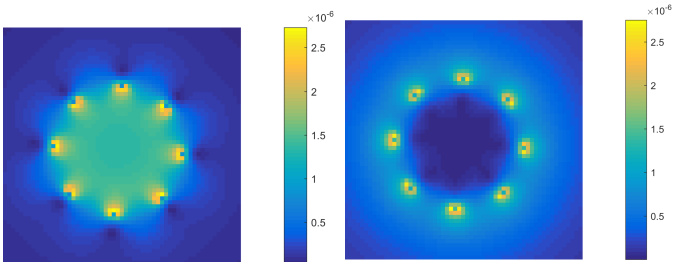

(a) B_1^+ (b) B_1^-

Fig. 5: B_1^+ and B_1^- at a frequency of 167 MHz of the MRI scanner studied in Section III.A.

A. Birdcage coil

The high-pass birdcage coil studied in this work has been depicted in Fig. 3(a) (one unit cell) and Fig. 3(b) (the whole mesh), with the passive capacitors in green and the exciting ports in red. It has 8 legs, a radius of 8 cm, a height of 15 cm and the width of the legs and the rings is 1 cm. The capacitors placed in the upper and lower rings between every leg, in the upper and lower rings are designed with a capacitance of 11 pF. Metal is considered as perfectly conducting in these examples. The mesh of one unit cell and the complete mesh are represented in Fig. 3(a) and Fig. 3(b) respectively. The birdcage is excited at two ports, separated by 90 degrees and with a 90 degrees phase shift, in order to selectively excite the B_1^+ field.

The method of moments usually requires the computation of the impedance matrix between basis and testing functions for every frequency. However, the computation time of this technique can be reduced using interpolation techniques [18]. The phase term of the impedance matrix that directly depends on the frequency can be extracted, obtaining in that way a smoother function that can be interpolated from impedance matrices that are computed just at a few frequencies. The scattering parameters that characterize the birdcage are computed twice. In the first numerical experiment, the impedance matrices are computed at just three frequencies and then they are interpolated with the method cited above. In the second one, they are computed for every 0.5 MHz, at 200 frequencies. As can be checked in Fig. 4, the results are very similar in both cases. The reduction in time is quite notable considering that just 3 impedance matrices have been computed over a wide frequency band and that the interpolation time is negligible.

The scattering parameters in Fig. 4 show a resonance frequency at 169 MHz. The resonance frequency of the birdcage without shielding and phantom is generally lower than the one of the whole system [19]. That is why it is advantageous to design the birdcage with a lower resonance frequency that the desired resonance frequency of the full scanner. Matching is not a primary concern in the first steps of the design as it is usually achieved later using matching circuits. The field distributions are shown in Fig. 5 at a frequency of 169 MHz. The B_1^+ field shows a good homogeneity in the area of interest and the B_1^- shows a low value in the same area. These characteristics are desired in MRI operation for obtaining homogeneous images.

B. Birdcage coil with metallic shielding and dielectric phantom

In the second example, the MRI analysis is expanded, including a metallic shielding and a dielectric phantom in addition to the birdcage. The birdcage is the same as in the previous example. The metallic shielding has a radius of 10 cm and a length of 15 cm. The dielectric cylinder is designed to mimick a human body part like an arm: it has a radius of 6 cm and a height of 20 cm, its permittivity is $\epsilon_r = 61$ and the conductivity is $\sigma = 0.8\ S/m$. The meshes of the unit cell and

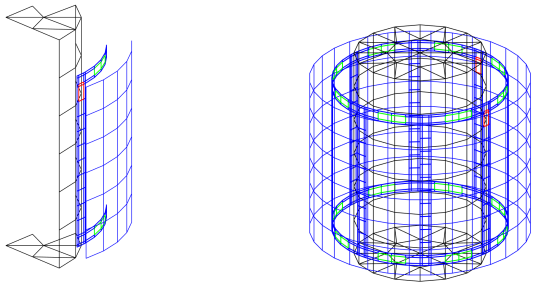

(a) Unit cell (b) Complete mesh

Fig. 6: Representation of the mesh of the example III.B.

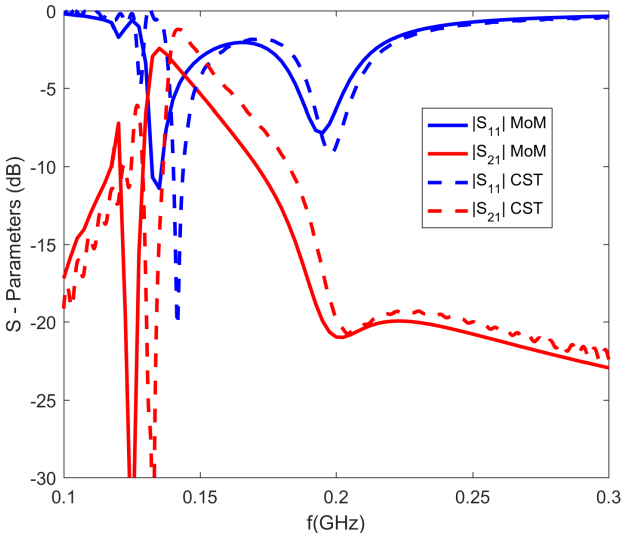

Fig. 7: Scattering parameters for the example described in Section III.B. Computed with the present method and with the commercial software CST.

of the whole scanner are represented in Fig. 6 (a) and Fig. 6 (b) respectively.

The scattering parameters are shown in Fig. 7. They are computed with the present method and with the commercial software CST. Both methods show similar results although there is a small shifting of $3-4$ MHz. It can be observed that the resonance frequency has shifted to 200 MHz. It can also be observed as the losses on the dielectric material are clearly present in the scattering parameters. The fields distribution at a frequency of 198 MHz is shown and validated using the commercial software CST in Fig. 8. A very good agreement can be seen: the error level is around 10% within the phantom, which is good considering that the birdcage is resonant at that frequency, so that a small change in the inputs may produce large changes in the outputs. The B_1^+ field shows a good homogeneity in the area of interest and the B_1^- shows a low value in the same area. However, due to the effect of the phantom, the fields are not as homogeneous as in the case of the previous example. This effect becomes more problematic when the frequency or the size of the sample are increased.

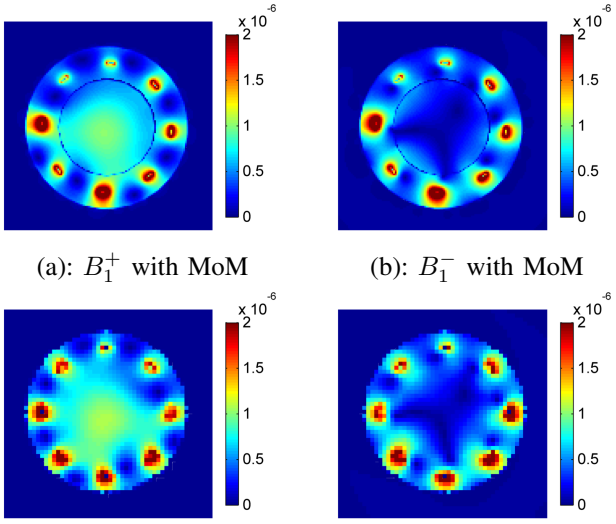

(a): B_1^+ with MoM (b): B_1^- with MoM

(c): B_1^+ with CST (d): B_1^- with CST

Fig. 8: Map of the B_1^+ (a,c) and B_1^- (b,d) fields at a frequency of 198 MHz inside the MRI scanner studied in Section III.B. Computed with the Method of Moments (a,b) and with the commercial software CST (c,d).

A last note concerns the time and resources required for the simulations. The MoM code accelerated using the ASM and the frequency interpolation were run on a computer equipped with a i7-3770 CPU. The code is not parallelized, so that it was running on a single core. The simulation of the full birdcage with the shielding and the phantom took between 11 and 12 minutes. More than 90% of the time is devoted to the computation of the impedance matrix, which is "embarrassingly parallelizable" and can therefore be strongly accelerated using more cores. For the same geometry, the CST simulations require 40 minutes using four cores on a i7-6700 CPU (20 minutes per input port). In both cases, the required RAM was similar (about 500 MB). In summary, using the non-parallelized version of the MoM, a speed-up factor of more than 3 can be achieved, while a parallelized version run on 4 cores could theoretically provide an additional speed-up factor of 3.

IV. Conclusion

An efficient analysis of MRI antennas using the method of moments is proposed. Exploiting the N^{th} order symmetry inherent to MRI antennas, shielding and phantoms, the array scanning method is adapted to the PMCHWT approach to deal with dielectric objects. Decreasing the complexity of the matrix filling by a factor of N and the solution time by a factor of N^2. Further improvements are made to enhance the performance and lower the computational cost, such as interpolation over frequencies.

ACKNOWLEDGMENT

This project has received funding from the European Union Horizon 2020 research and innovation program under grant agreement No. 736937.

REFERENCES

[1] F. Bloch, W. W. Hansen, and M. Packard, "Nuclear Induction", *Phys. Rev.*, vol. 69, p. 127, 1946.

[2] E. M. Purcell, H. C. Torrey, and R. Pound, "Resonance absorption by nuclear magnetic moments in a solid", *Phys. Rev.*, vol. 69, p. 37, 1946.

[3] E. D. Becker, "A Brief History of Nuclear Magnetic Resonance", *Anal. Chem.*, vol. 65, no. 6, p. 295302, March 1993.

[4] Y. Zhu, "Parallel excitation with an array of transmit coils", *Magnetic Resonance in Medicine*, vol. 51, p. 775-784 Apr 2004.

[5] M. J. Freire, R. Marques, L. Jelinek. "Experimental demonstration of a $\mu = 1$ metamaterial lens for magnetic resonance imaging", *Applied Physics Letters*, 93, 231108, 2008.

[6] J.van Gemert, W.M.Brink, A.G.Webb and R.F.Remis, "An efficient methodology for the analysis of dielectric shimming materials in Magnetic Resonance Imaging", *IEEE Trans. Med. Imag.*, vol. 36, no. 2, pp. 666-673, 2016.

[7] C. E. Hayes et al., "An efficient, highly homogeneous radiofrequency coil for whole-body NMR imaging at 1.5 T", *Journal of Magnetic Resonance*, Vol. 63, Issue 3, July 1985, pp 622-628, 1969.

[8] J. M. Jin, R. L. Magin, G. Shen, and T. Perkins, "A Simple Method to Incorporate the Effects of an RF Shield into RF Resonator Analysis for MRI Applications", *IEEE Trans. Biomed. Eng.*, pp. 840-843, 1995.

[9] Jian-Ming Jin, "Electromagnetics in magnetic resonance imaging", *IEEE Antennas and Propagation Magazine*, vol. 40, no. 6, pp. 7-22, Dec 1998.

[10] J. F. Villena et al., "Fast Electromagnetic Analysis of MRI Transmit RF Coils Based on Accelerated Integral Equation Methods", *IEEE Transactions on Biomedical Engineering*, vol. 63, no. 11, pp. 2250-2261, Nov. 2016.

[11] M. Kozlov, R. Turner, "Fast MRI coil analysis based on 3-D electromagnetic and RF circuit co-simulation", *Journal of Magnetic Resonance*, pp 147152, 2009.

[12] M. A. Carr, J. L. Volakis and D. Ross, "Acceleration of free-space discrete body of revolution codes by exploiting circulant submatrices", *IEEE Transactions on Antennas and Propagation*, vol. 50, no. 9, pp. 1319-1322, Sep 2002.

[13] R. Sarkis, C. Craeye, "Circular array of wideband 3D Vivaldi Antennas", *URSI International Sympusium on Electromagnetic Theory*, 2010

[14] A. Roederer, "Etude des réseaux finis de guides rectangulaires à parois épaisses", *L'onde électrique*, vol 51, 854-861, Nov 1971.

[15] B. A. Munk and G. A. Burrell, "Plane-wave expansion for arrays of arbitrarily oriented piecewise linear elements and its application in determining the impedance of a single linear antenna in a lossy half-space", *IEEE Trans Antennas Propagat.* vol 27, 331-343, 1979.

[16] F. Capolino, D. R. Jackson, D. R. Wilton , "Fundamental Properties of the Field at the Interface Between Air and a Periodic Artificial Material Excited by a Line Source", *Electromagnetics* vol 10, Jan 2005.

[17] S. M. Rao, D. R. Wilton , "E-field,H-field,and combined field solution for arbitrarily shaped three-dimensional dielectric bodies", *IEEE Trans Antennas Propagat.* pp 407421, 1990.

[18] E. H. Newman, "Generation of Wide-Band Data from the Method of Moments by Interpolating the Impedance Matrix", *IEEE Trans Antennas Propagat.* vol 36, 1820-1824, Dec 1988.

[19] T.S. Ibrahim, R. Lee, B.A. Baertlein, Y. Yu and P.M.L. Robitaille, "Computational analysis of the high pass birdcage resonator: finite difference time domain simulations for high-field MRI", *Magnetic Resonance Imaging*, vol. 18, no. 7, pp. 835-843, 2000.